Tunable terahertz quantum cascade lasers with external gratings

Citation: Lee, Alan Wei Min, Benjamin S. Williams, Sushil Kumar, Qing Hu, and John L. Reno. "Tunable Terahertz Quantum Cascade Lasers with External Gratings." Optics Letters 35, no. 7 (April 1, 2010): 910. © 2010 Optical Society of America

As Published: http://dx.doi.org/10.1364/OL.35.000910

Publisher: Optical Society of America

Persistent URL: http://hdl.handle.net/1721.1/86361

Version: Final published version: final published article, as it appeared in a journal, conference proceedings, or other formally published context

Tunable terahertz quantum cascade lasers with external gratings

Alan Wei Min Lee,[1,*] Benjamin S. Williams,[2] Sushil Kumar,[1] Qing Hu,[1] and John L. Reno[3]

[1]*Department of Electrical Engineering and Computer Science and Research Laboratory of Electronics, Massachusetts Institute of Technology, Cambridge, Massachusetts 02139, USA*

[2]*Current address: Department of Electrical Engineering, University of California at Los Angeles, Los Angeles, California 90095, USA*

[3]*CINT, Sandia National Laboratories, Department 1132, MS 1303, Albuquerque, New Mexico 87185, USA*

**Corresponding author: awmlee@mit.edu*

Received October 29, 2009; revised January 12, 2010; accepted January 15, 2010; posted February 19, 2010 (Doc. ID 118968); published March 18, 2010

We demonstrate a frequency tunable external cavity terahertz quantum cascade laser using an abutted antireflection-coated silicon lens to reduce facet reflection and as a beam-forming element, with an external grating providing frequency selective optical feedback. Angle tuning of the grating allows a single longitudinal mode of the laser ridge to be selected, resulting in discontinuous tuning over a 165 GHz range around a center frequency of 4.4 THz. Another device exhibited 145 GHz of total tuning with 9 GHz of continuous tuning near the longitudinal modes of the laser. © 2010 Optical Society of America

OCIS codes: 140.3070, 140.3600.

Terahertz quantum cascade lasers (THz QCLs) now emit over a range of 1.2–4.9 THz [1,2] and are highly desirable as single mode tunable radiation sources for spectroscopy and as local oscillators for heterodyne detection [3,4]. Electrical tuning using the temperature dependence of refractive index [5] or the cavity-pulling effect [6,7] produces a relatively small fractional tuning (<1%) and is not suitable for spectroscopy of solid features (>100 GHz). For this application an external cavity (EC) laser with frequency selective feedback can be used to take advantage of the broad gain bandwidth of THz QCLs, which have shown simultaneous lasing spectra spanning >600 GHz [5]. Initial approaches to tuning EC-QCLs had limited success owing to poor antireflection (AR) coatings, resulting in the inability to suppress optical feedback from the cleaved facets [8]. Improved AR coatings were demonstrated in [9] using a single layer of SiO_2 with an index of refraction, $n_{SiO_2} \approx 1.8-1.9$, which is nearly ideal for a $\lambda/4n$ impedance matching layer where $n = \sqrt{n_{GaAs}} \approx 1.89$. The reflectivity of coated facets was estimated to be <4%, which was sufficient for external cavity operation using a closely spaced broadband metallic reflector inside the cryostat. Continuous tuning was demonstrated by adjusting the distance to the facet, but it was restricted to a free spectral range of the cavity (~15 GHz) owing to a lack of frequency selectivity.

In this Letter, we describe an EC-QCL whose cleaved front facet is optically coupled to a silicon hyperhemispherical lens with an external grating for optical feedback (Fig. 1). Two external cavity configurations were used and achieved similar results: a large 10 mm diameter lens for direct collimation of the emitted beam [Fig. 1(a)], and a smaller 3 mm diameter lens used with an off-axis parabolic mirror for beam collimation [Fig. 1(b)]. While the use of the larger lens reduces the number of optical components, the positioning of the smaller lens is less sensitive to thermal contraction. The QCLs are based on the resonant-phonon depopulation design and use a semi-insulating surface plasmon waveguide as described in [10]. Two devices were used in the configuration Fig. 1(a) with dimensions of 100 μm wide by 1.34 and 1.5 mm long, and a device measuring 150 μm wide by 1.25 mm long was used in configuration Fig. 1(b). High resistivity silicon (HRSi, >10 k Ω) lenses and thin HRSi spacers were abutted to the cleaved laser facets [11]. For the larger 10 mm diameter lens a spring retaining clip was used to maintain contact with the spacer/facet. For the

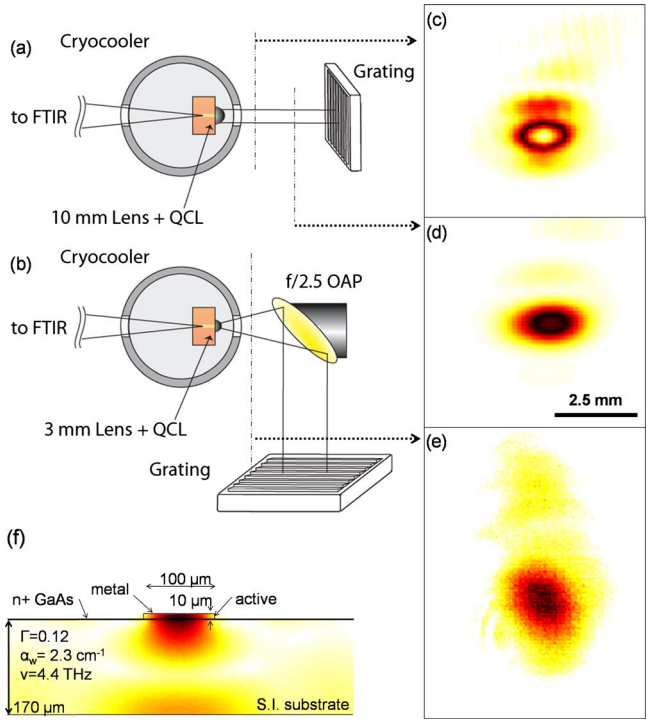

Fig. 1. (Color online) (a), (b) External-QCL configurations with and without off-axis paraboloid mirror (OAP). (c)–(e) Measured beam patterns from lens coupled QCLs. (f) Calculated two-dimensional fundamental mode intensity.

0146-9592/10/070910-3/$15.00

smaller 3 mm lens, the holding force of Norland 81 UV-curing glue was sufficient to secure the lens and spacer. The 10 mm lens configuration was used with two slightly different hyperhemisphere lengths (measured tip-to-facet) of 7.21 and 6.97 mm for the 1.34- and 1.5-mm-long devices, respectively, which showed negligible performance differences. Collimation over the long, ~80 mm, distance between the lens and the grating is possible because of the large diameter lens, which leads to a large beam waist, w_o, and a correspondingly small Gaussian beam divergence angle, $\theta \approx \lambda/\pi w_o$. This was verified by imaging the beam from the 1.34-mm-long device at distances of 52 and 60 mm from the lens tip [Figs. 1(c) and 1(d)] [12]. By comparison, the much smaller 3 mm lens configuration has a smaller beam waist, and it cannot be collimated over appreciable distances. Instead the hyperhemisphere length is set to 1.96 mm, close to the $R+R/n_{\mathrm{Si}}$ aplanatic point, which reduces optical aberrations, where R and n_{Si} are the radius and index of the lens [13]. The diverging beam can be seen by the larger beam pattern at ~22 mm from the lens tip [Fig. 1(e)]. The echelle grating is operated in Littrow and is blazed for 118 μm (2.5 THz). The calculated reflectivity of the grating at 4.4 THz is 63% and 34% for the first and second orders, respectively (PC Grate, IIG).

The devices were mounted in a closed-cycle pulse-tube cryorefrigerator (PT60, Cryomech) and cooled to ~30 K. A pulsed electrical bias of 13.5 ms repeated at 20 Hz was used for the collected light versus current (L-I) characteristics in Fig. 2. In Fig. 2(a), three different cavity conditions are shown for the 1.34-mm-long device, showing increasing values of lasing threshold current density, J_{th}: without a lens, 600 A/cm^2; using a lens with maximum external feedback from a gold mirror, 650 A/cm^2; and using a lens with no external feedback, 710 A/cm^2. The increase in J_{th} corresponds to increased optical loss through lower reflectivities. This also results in decreases in slope efficiency at threshold (dP/dJ) as light is collected from the non-lens coupled facet whose reflectivity does not change. The maximum and minimum reflectivities of the external optical system can be determined by studying the effect of the cavity losses on J_{th}. For resonant-phonon designs J_{th} is limited by a parasitic current channel ($J_{th} > J_{\mathrm{Parasitic}}$) necessitating the incremental comparison of J_{th} with loss, $\Delta J_{th} \propto \Delta\alpha$, unlike the analysis presented in [9] where J_{th} was directly compared with losses due to the use of a bound-to-continuum design. Here, α is the sum of the optical loss terms: the waveguide loss, α_ω; the mirror loss from the output facet, α_{m1}; the effective mirror loss from the lens-coupled facet, α_{m2}, which includes residual reflection from the lens and any external feedback; and an additional loss, α_{add}, which can be added to the path of the external cavity to study J_{th}. Additional loss is added by inserting a number of angled polyester/polyethylene sheets in the external cavity. Transmission values, T, were determined by biasing the laser above threshold and measuring the transmitted power using a pyroelectric detector. Loss values are obtained using $\alpha_{\mathrm{add}} = -\log(T)/L$, where L is the device length. The inset of Fig. 2(a) shows the resulting linear relationship of J_{th} versus α_{add} with a slope of $d\alpha/dJ = 12(\pm 1.9) \times 10^{-2}[\mathrm{cm}^{-1}/(\mathrm{A/cm}^2)]$, allowing calculation of α_{m2},

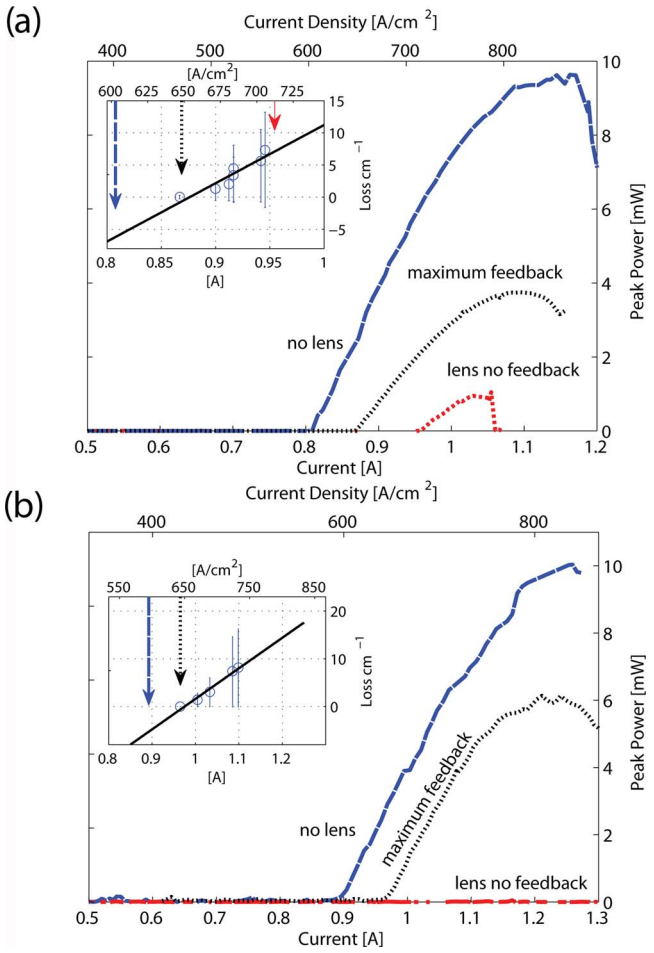

Fig. 2. (Color online) Collected light versus current characteristics for devices measuring 100 μm wide by (a) 1.34 mm long and (b) 1.5 mm long, using 10 mm diameter lens setup of Fig. 1(a). The insets show variation of threshold current versus additional loss added to the path of the maximum feedback external cavity. Vertical arrows indicate lasing threshold.

$$\alpha_{m2} = \frac{-\log(0.32)}{2L} + (J'_{th} - J_{th})\frac{\partial\alpha}{\partial J}, \qquad (1)$$

where the first term is the assumed mirror loss from a bare facet with a reflectivity of 32%, and the second term is the additional loss inferred by the increase in threshold current density, where J_{th} is measured without a lens and J'_{th} is measured with a lens and various amounts of feedback. For maximum external feedback, α_{m2} is 9.8 cm^{-1}, which corresponds to a reflectivity of 7.3(±1.3)%. For minimum external feedback, α_{m2} is 18 cm^{-1}, which corresponds to a minimum residual reflectivity of 1(±0.5)%. Similar measurements were performed on the 1.5-mm-long device, which showed better AR characteristics through suppression of lasing in the absence of exter-

nal feedback. The resulting slope is $d\alpha/dJ = 9.6(\pm 0.4) \times 10^{-2}$, corresponding to an α_{m2} of 8.5 cm^{-1} or 8.4(±0.2)% maximum reflectivity. An upper bound for the minimum reflectivity is determined using the highest observed threshold of 730 A/cm^2, resulting in residual reflectivity values of $<0.6(\pm 0.1)\%$.

The measured maximum reflectivity of 7%–8% using the gold external mirror can be compared with a calculated value of 20% resulting from optical and coupling losses in the EC: the polypropylene vacuum window has ~85% transmission, and the atmospheric transmission is ~90% for a 17 cm external path length at 296 K and 40% relative humidity (Fig. 3, HITRAN 2008). The AR coating on the HRSi lens is a 13-μm-thick low-density polyethylene (LDPE) layer with a transmission of ~83% at 4.4 THz (Fig. 3) when double side coated on a 1.5-mm-thick HRSi window. Similar results were obtained for a 10-μm-thick Parylene-N layer; however, LDPE was chosen for its simplified application by a temperature-controlled hot air gun. Coupling losses arise due to the imperfect overlap of the fundamental waveguide mode [shown in Fig. 1(f)] with the optical feedback from external optics, which inverts the image of the mode due to beam collimation at the grating. A coupling value of ~40% is calculated from an overlap integral of the mode with an inverted version of itself. This asymmetry can be seen in the beam images of Figs. 1(c)–1(e). Additional losses include optical aberrations and misalignment, which are not calculated here.

Grating angle adjustment results in the tuning spectra shown in Fig. 3(b) for the 1.5- and 1.25-mm-long devices, operated with pulses of 200–800 ns at 100 kHz. For the 1.5-mm-long device [Fig. 3(a)] the tuning range is 165 GHz or 3.8% of the 4.4 THz center frequency. Frequency hopping is observed between the longitudinal modes of the device spaced at 24 GHz (n_{eff}=4.24). Even though lasing is suppressed in the absence of feedback, the lens does not provide a perfect AR coating, and lasing occurs on the longitudinal modes where there is some small residual feedback in addition to the external feedback. The 1.25-mm-long device [Fig. 3(b)] showed 145 GHz of discontinuous tuning between modes spaced at 29 GHz (n_{eff}=4.14). However, in this case, 9 GHz of continuous tuning near the longitudinal modes was measured, suggesting either slightly stronger feedback or a better AR effect of the lens.

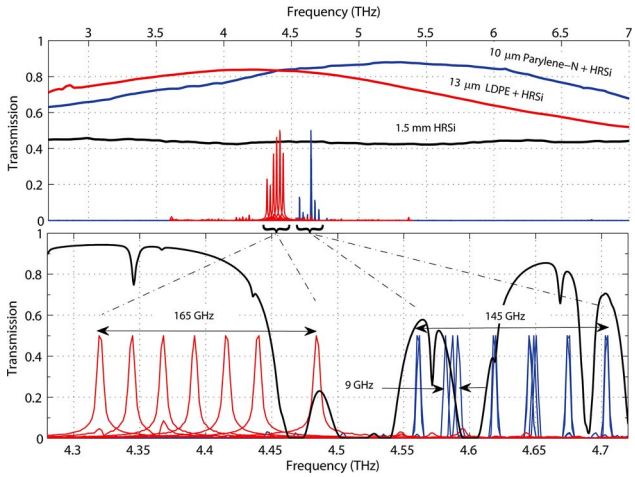

Fig. 3. (Color online) (a) Transmission spectra of antireflection coatings applied to both sides of a 1.5-mm-thick HRSi window. Unnormalized QCL spectra of devices measuring 100 μm wide by 1.5 mm long [light gray (red online)] and 150 μm wide by 1.25 mm long [dark gray (blue online)]. (b) Enlarged and normalized spectra from (a) and calculated atmospheric transmission through external cavity (HITRAN 2008).

This work has shown coarse single mode tuning of over 165 GHz, which is sufficient for measurement of the broad spectral features of solids. Improved tuning will be possible with stronger optical feedback, and a vertically symmetric waveguide. Amplifiers based on the EC-QCL are possible using an external signal instead of external feedback.

This work is supported by the Air Force Office of Scientific Research, National Aeronautics and Space Administration (NASA), and National Science Foundation (NSF). Sandia is a multiprogram laboratory operated by Sandia Corporation, a Lockheed Martin Company, for the United States Department of Energy's National Nuclear Security Administration under contract DE-AC04-94AL85000.

References

1. C. Walther, M. Fischer, G. Scalari, R. Terazzi, N. Hoyler, and J. Faist, Appl. Phys. Lett. **91**, 131122 (2007).
2. A. W. M. Lee, Q. Qin, S. Kumar, B. S. Williams, Q. Hu, and J. L. Reno, Appl. Phys. Lett. **89**, 141125 (2006).
3. A. A. Danylov, J. Waldman, T. M. Goyette, A. J. Gatesman, R. H. Giles, J. Li, W. D. Goodhue, K. J. Linden, and W. E. Nixon, Opt. Express **16**, 5171 (2008).
4. J. R. Gao, J. N. Hovenier, Z. Q. Yang, J. J. A. Baselmans, A. Baryshev, M. Hajenius, T. M. Klapwijk, A. J. L. Adam, T. O. Klaassen, B. S. Williams, S. Kumar, Q. Hu, and J. L. Reno, Appl. Phys. Lett. **86**, 244104 (2005).
5. S. Kumar, B. S. Williams, Q. Qin, A. W. M. Lee, Q. Hu, and J. L. Reno, Opt. Express **15**, 113 (2007).
6. L. A. Dunbar, R. Houdre, G. Scalari, L. Sirigu, M. Giovannini, and J. Faist, Appl. Phys. Lett. **90**, 141114 (2007).
7. H. Zhang, L. A. Dunbar, G. Scalari, R. Houdré, and J. Faist, Opt. Express **15**, 16818 (2007).
8. J. Hensley, D. Bamford, M. Allen, J. Xu, A. Tredicucci, H. Beere, and D. Ritchie, in *Optical Terahertz Science and Technology*, Technical Digest Series (Optical Society of America, 2005), paper TuA3.
9. J. Xu, J. M. Hensley, D. B. Fenner, R. P. Green, L. Mahler, A. Tredicucci, M. G. Allen, F. Beltram, H. E. Beere, and D. A. Ritchie, Appl. Phys. Lett. **91**, 1 (2007).
10. B. S. Williams, S. Kumar, Q. Hu, and J. L. Reno, Electron. Lett. **42**, 89 (2006).
11. A. W. M. Lee, Q. Qin, S. Kumar, B. S. Williams, Q. Hu, and J. L. Reno, Opt. Lett. **32**, 2840 (2007).
12. A. W. M. Lee, B. S. Williams, S. Kumar, Q. Hu, and J. L. Reno, IEEE Photon. Technol. Lett. **18**, 1415 (2006).
13. M. Born and E. Wolf, *Principles of Optics* (Pergamon, 1959).